dx.doi.org/10.14227/DT190412P6

Permeation Kinetics Studies of Physical Mixtures of Artemisinin in Polyvinylpyrrolidone

e-mail: gmdogar356@gmail.com

Syed Nisar Hussain Shah[1], Yasser Shahzad[2], Muhammad Tayyab Ansari[1], Muhammad Haneef[3], Madeeha Malik[3], Amir Badshah[4], and Ghulam Murtaza[5,*]

[1]*Faculty of Pharmacy, Bahauddin Zakariya University, Multan, Pakistan*

[2]*Division of Pharmacy and Pharmaceutical Sciences, School of Applied Sciences, University of Huddersfield HD1 3DH, UK*

[3]*SNS Pharmaceutical Research Laboratory, Multan, Pakistan*

[4]*Department of Pharmacy, Peshawar University, Peshawar, Pakistan*

[5]*Department of Pharmaceutical Sciences, COMSATS Institute of Information Technology, Abbottabad, Pakistan*

ABSTRACT

Artemisinin (ART), the parent compound of a novel family of antimalarial drugs, was used as a model drug that is lipophilic and has low bioavailability (32%) after oral delivery. The primary objective was to study the effect of polyvinylpyrrolidone (PVP) on the permeation enhancement and solubility of physical mixtures (PM) of ART in PVP–K30 in various solvent systems (i.e., distilled water, phosphate buffered saline [PBS], and methanol). PMs of drug–PVP in 1:0.5, 1:1, 1:2, 1:4, and 1:9 ratios were prepared by simple mixing in a mortar and pestle. Fourier transform infrared (FTIR) spectrophotometry and X-ray powder diffraction (XRPD) were applied to characterize the PMs. The solubility of ART was investigated at 37 ± 0.5 °C in three solvents. Permeation of ART-saturated solutions across a silicone membrane in Franz diffusion cells was studied using Fick's law of diffusion. FTIR and XRPD studies have shown some interactions, and there was a phase change of artemisinin from crystalline to amorphous form as the concentration of PVP–K30 in PM ratios increased. Solubility order increased with an increase in PVP–K30 concentration for the water–PBS solvent system, while in methanol, it was erratic. Flux rate and permeability coefficient were enhanced with an increase in PVP–K30 concentration. In less permeable solvents like water and PBS, the enhancement ratio was high, while the enhancement ratio was low in a highly permeable solvent like methanol. In conclusion, with an increase in concentration of PVP, the permeation rate and solubility of ART increased.

INTRODUCTION

The concept of percutaneous absorption given by Stoughton (*1*) in 1965 has opened a new horizon of knowledge in drug delivery techniques and has thus paved the way for the development of transdermal drug delivery (TDD) products. Transdermal drug delivery facilitates the passage of therapeutic quantities of drug substances through skin into the general circulation for their systemic effects, thus bypassing the hepatic first-pass effect. Drug delivery through the cutaneous route has several advantages over other drug delivery routes. However, this route faces a major problem presented by the barrier function of the skin in which the stratum corneum plays a vital role (*1*).

To overcome this passive barrier system, chemical permeation enhancers (CPE) that temporarily lower the impermeability of skin and facilitate the absorption of drug through skin are extensively used. The physical and chemical properties should be kept in mind while selecting a CPE (*2*). In recent years, different types of penetration enhancers such as terpenes, pyrrolidones, alcohols, glycols, fatty acids, esters, and sulfoxides have been successfully utilized to decrease the barrier function of the stratum corneum (*3*).

Artemisinin (ART) is a parent compound of novel family of antimalarials. It is extracted from a Chinese traditional plant *Artemisia annua*, L. Asteraceae. ART is very effective against the malaria parasite, including the multidrug-resistant falciparum species (*4*). It was first isolated and characterized as active compound by Chinese scientists in 1972. Since then it has been successfully utilized as an antimalarial drug (*5*). It is extensively metabolized in the liver, thus oral bioavailability is low (*6*). Its low molecular weight (MW 282.3) and log *P* (octanol–water partition coefficient) value of 2.95 make it a suitable candidate for transdermal drug delivery.

Polyvinylpyrrolidone (PVP) is a water-soluble polymeric compound composed of repeating units of *N*-vinylpyrrolidone (monomer). PVP–K30 is well tolerated physiologically, is readily soluble in water, and is used for increasing the dissolution and oral absorption of many water-insoluble drugs (*7*, *8*). A previous study on enhancement of the dissolution and permeation profile of meloxicam, a poorly water-soluble drug, has shown some successful results using PVP–K30 (*9*).

This study describes the solid-state properties of different physical mixture ratios of ART in PVP–K30 by applying techniques like FTIR and X-ray powder diffraction (XRPD). The effect of PVP–K30 on the solubility of ART and its role as a permeation enhancer was explored in detail by

*Corresponding author.

studying the in vitro diffusion properties of PMs of ART in PVP–K30. Franz diffusion cells were used to determine the permeation parameters.

MATERIALS AND METHODS

Chemicals

The following chemicals were used: artemisinin (ART) 99.9% purity (Alchem, New Dehli, India); PVP–K30) (China); HPLC grade methanol and potassium dihydrogen phosphate (Merck, Darmstadt, Germany); toluene and disodium hydrogen phosphate (Fischer Scientific Chemicals, Germany); sodium chloride and potassium chloride (Aldrich, USA); and vacuum grease (Dow Corning, USA).

Preparation of Physical Mixtures

Physical mixtures were prepared by mixing different ratios of ART and PVP–K30 (1:0.5, 1:1, 1:2, 1:4, and 1:9) thoroughly in a dried glass mortar and pestle for about 5–10 min until a homogeneous mixture was obtained (10). These ratios were designated as R_1, R_2, R_3, R_4, and R_5, respectively.

Artemisinin Assay

The concentration of ART was measured by slightly modifying the method described by Zhao and Zeng (*11*), in which ART is transformed into a UV-absorbing compound with an absorbance maximum at 290 nm by heating in a 0.2% NaOH solution.

Aliquots (1 mL) of each dilution were placed in separate test tubes; 5 mL of 0.2% NaOH solution was added to each, then heated at 50 ± 1 °C for 30 min and allowed to cool in a refrigerator. The absorbance of each sample was measured at 290 nm with a UV spectrophotometer (Agilent 2005, Germany), and a calibration curve was obtained.

Solubility Studies

The solubilities of pure ART as well as each PM were determined in each of the examined solvent systems (i.e., distilled water [pH 6.8 ± 0.1], PBS, and methanol) by stirring an excess quantity of each compound (PM ratios) with the relevant solvent for 48 h at a constant temperature of 37 ± 0.5 °C. The suspensions were then centrifuged at 4000 rpm for 30 min, and an aliquot of the supernatant was taken out by micropipette and analyzed spectrophotometrically at 290 nm to determine the concentration in µg/mL.

Fourier Transform Infrared Spectrophotometry

Fourier transform infrared (FTIR) spectral measurements were performed using a 2400S Spectrometer (Schimadzu, Japan) employing the KBr disc method. The samples were scanned over the range of 450–4000 cm^{-1}.

X-ray Powder Diffraction

XRPD for each ratio of PM was performed using a D8 Discover (Bruker, Germany) apparatus (*11*). Measurement conditions included target (CuKα), voltage (35 KV), and current (35 mA). A system of diverging, receiving, receiving, and antiscattering slits of 1°, 1°, 1°, and 0.15°, respectively, was used. Eva software was used for data processing (Evaluation Package, Bruker, Germany). Patterns were obtained using scan speed of 4°/min with 2θ between 5° and 50°.

In Vitro Permeation Studies Across Silicone Membrane

Diffusion studies of the selected permeants across a silicone membrane (300 µm) were performed using Franz-type diffusion cells (*12*, *13*). Silicone membrane was purchased from Inza Scientific Distributors, Pakistan. The mode of transport through a silicone membrane is similar to that for the stratum corneum (*13*). Before the commencement of a permeation experiment, water was used to ensure membrane integrity by evaluating the water permeability coefficient, an indicator of barrier function. Cells used in this study had a receptor phase of about 5 mL and a diffusional area of approximately 0.788 cm^2. Sheets of silicone membrane were cut to the appropriate size in a round shape and were soaked overnight in the receptor solution. The membrane was then placed between the two compartments of the diffusion cells. Vacuum grease was used to produce a leak-proof seal between the membrane and the two compartments of the diffusion cells.

The receptor compartment was filled with phosphate buffered saline (PBS) at pH 7.4, which is close to skin pH. To remove air bubbles and to prevent the buildup of air pockets in the receptor phase, PBS was degassed in an ultrasonic bath. To prevent evaporation from the receptor compartment, the cell arm was covered with Parafilm. Uniform mixing of the receptor phase was obtained with a magnetic stirrer that was placed in the receptor compartment. The diffusion cells were placed on a stirring bed immersed in a water bath at 37 ± 0.5 °C to maintain the temperature of the membrane surface. After 1 h, the receptor phase was completely removed and refilled with preheated PBS.

The saturated control solutions were designated C_1 for pure ART in water, C_2 in PBS, and C_3 in methanol. The saturated solutions of physical mixture were designated as R_w, R_{PBS}, and R_{me} with the corresponding ratio. The donor compartment was charged with 1 mL of saturated solution with excess solute present to maintain the saturation throughout the experiment. This ensured that the depletion of solute in the vehicle did not become the rate-limiting step in diffusion. After elapsed times of 5, 15, 30, 45, 60, 90, 120, and 180 min, 0.2-mL samples were withdrawn from the receptor solution (PBS) using micropipettes, followed by addition of the same volume of preheated receptor solution to maintain sink conditions. The samples were analyzed spectrophotometrically at 290 nm to obtain the amount permeated through the silicon membrane. Experiments were conducted in triplicate to obtain statistically significant data.

Table 1. Solubilities and Solubility Enhancement Ratios (ER_{sol}) of PM Ratios in Different Solvents

	Water		PBS		Methanol	
Sample	Solubility (µg/mL)	ER_{sol}	Solubility (µg/mL)	ER_{sol}	Solubility (µg/mL)	ER_{sol}
C	12.9	-	15.65	-	163.6	-
R_1	16.4	1.27	15.9	1.01	117.82	0.72
R_2	17.98	1.4	17.15	1.09	552	3.4
R_3	26.56	2.05	24.56	1.56	231.15	1.4
R_4	31.32	2.42	37.23	2.37	189.4	1.2
R_5	34.81	2.7	46.73	2.98	114.9	0.7

Statistical Analysis

All the results presented here are expressed as mean ± SD ($n = 3$) except for the solubility results. One-way ANOVA with $p < 0.05$ was performed to check the significance of the obtained values.

RESULTS AND DISCUSSIONS

Solubility Studies

The solubility of ART from each PM in various solvents was compared with the solubility of pure ART in the same solvents; solubility data and the corresponding solubility enhancement ratios (ER_{sol}) are summarized in Table 1. The solubility of PMs in water and PBS increased as the fraction of PVP–K30 increased, and ART solubility from PMs in water and PBS showed similar values. The lowest solubilities of ART were seen at ratio R_1 (16.4 µg/mL in water and 15.9 µg/mL in PBS). At ratio R_5, the solubility of ART was highest (34.81 µg/mL in water and 46.73 µg/mL in PBS). However, the results for the solubility of ART from PMs in methanol are significantly different ($p < 0.05$) in the sense that the trend of increasing behavior was not maintained. Ratio R_2 showed maximum solubility (552 µg/mL), and R_5 showed the least solubility (114.9 µg/mL). The effect of PVP–K30 on the solubility is described in terms of solubility enhancement ratios (ER_{sol}) as shown in Table 1. The ER_{sol} shows the extent to which the solubility was affected by the concentration of PVP in the three solvents examined. The highest values of solubility were observed for R_5 in water (34.81 µg/mL) and in PBS (46.73 µg/mL) with ER_{sol} of 2.7- and 2.98-fold, respectively. The maximum solubility for PM in methanol was observed at the ratio R_2 with a 3.4-fold increase in solubility over that of the control.

Fourier Transform Infrared Spectrophotometry

The interaction between drug and carrier often leads to identifiable changes in the FTIR profile. FTIR spectra of different ratios of physical mixtures of ART in PVP–K30 were compared with the standard spectra of ART and PVP–K30 as shown in Figure 1. In the functional group region, band shifting was observed in O–H stretching at 3885 cm^{-1} for the ratio R_5, 3382 cm^{-1} for R_4, 3377 cm^{-1} for R_3, 3381 cm^{-1} for R_2, and 3380 cm^{-1} for R_1. A shift was seen for CH at 2956 cm^{-1} for R_5, 2950 cm^{-1} for R_4, 2950 cm^{-1} for R_3, 2954 cm^{-1} for R_2, and 2950 cm^{-1} for R_1. The carbonyl stretching was seen at 1637 cm^{-1} for R_5, 1640 cm^{-1} for R_4, 1647 cm^{-1} for R_3, 1637 cm^{-1} for R_2, and 1654 cm^{-1} for R_1.

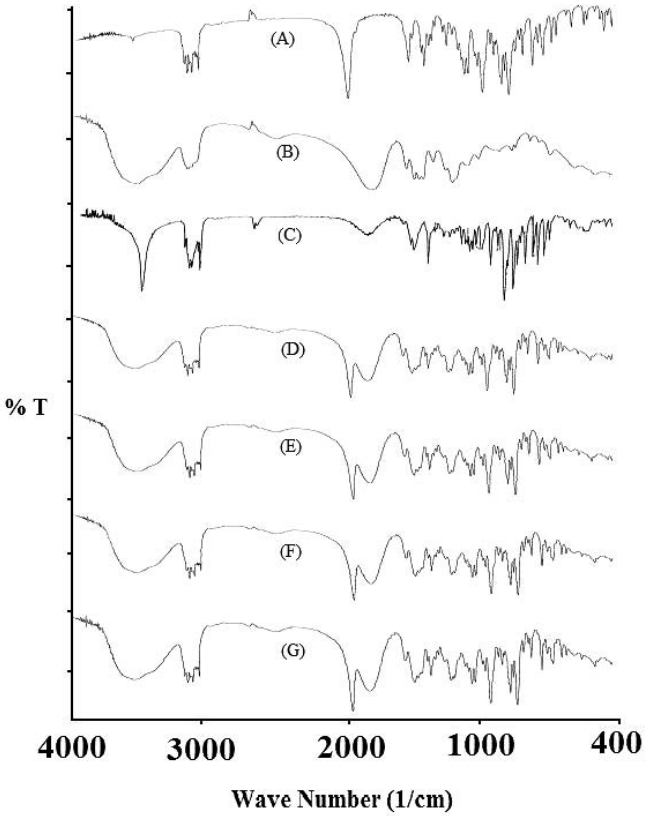

Figure 1. FTIR spectra of (A) pure ART, (B) PVP–K30, (C) R_1, (D) R_2, (E) R_3, (F) R_4, and (G) R_5.

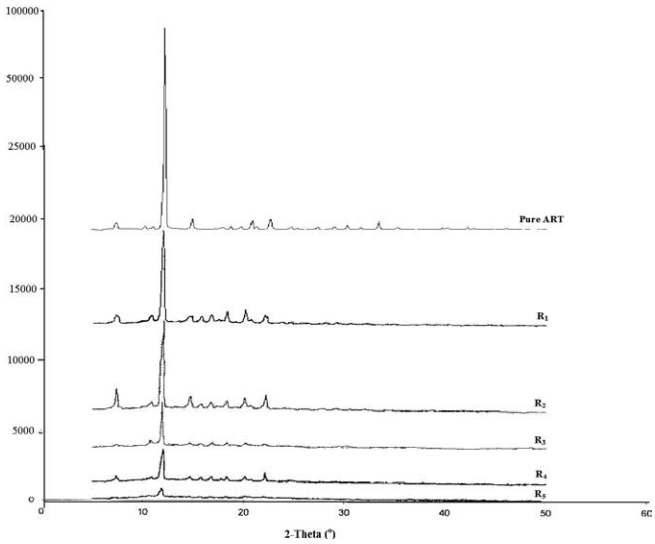

Figure 2. XRPD patterns of pure ART and PM in ratios R_1, R_2, R_3, R_4, and R_5.

In the fingerprint region, a shift was exhibited in the C–O stretch at 1093 cm^{-1} with comparatively shorter peaks for pure artemisinin, and no shifts were observed at 1093 cm^{-1} for the all the physical mixture ratios. In addition, the band at 876 cm^{-1} (O–O–C linkage), which is characteristic of artemisinin, was observed without shifting, while the band at 824 cm^{-1} (O–O stretching in chair form) disappeared in physical mixtures, which confirms interaction. A shift in C–N stretching was not observed in any of the physical mixture ratios. FTIR spectra revealed that the interaction between artemisinin and PVP–K30 was enhanced with an increase in the polymer concentration. The presence of N–H and C=O peaks in addition to artemisinin peaks in the spectra of physical mixtures indicates stronger interactions between drug and carrier. These interactions became stronger as the concentration of PVP–K30 was increased.

X-ray Powder Diffraction

Figure 2 displays the XRPD patterns of pure ART and PMs. ART is a highly crystalline powder with characteristic sharp peaks at 2θ diffraction angles of 7.21°, 11.96°, 14.54°, 20.24°, 21.92°, and 32.27°. The peak appearing at 2θ of 11.96° is the most prominent. XRPD data of ART in PM with PVP–K30 still shows crystallinity, but the crystallinity decreased gradually with increasing ratio of PVP–K30 as shown by the XRPD patterns of PM ratios from R_1 to R_5. The PM ratio R_5 shows a marked decrease in the crystallinity of ART, which shows a strong influence of PVP–K30 on the physical state of ART. XRPD patterns of physical mixtures show a gradual decrease in peak intensity (characteristic peaks of ART) as a function of PVP–K30 concentration, indicating a phase change from crystalline to amorphous, similar to dihydroartemisinin (*11*) and meloxicam (*9*).

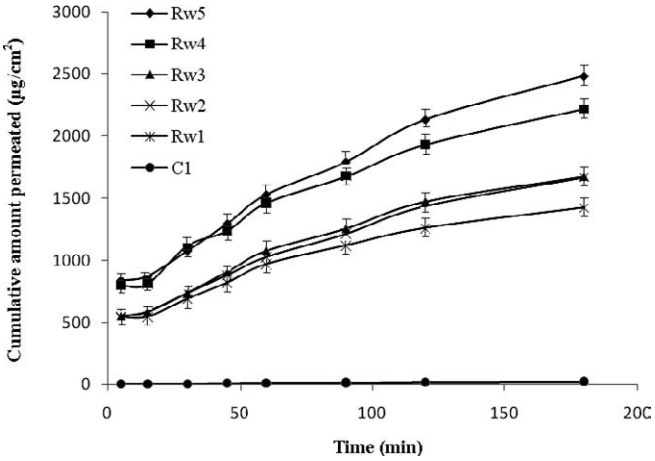

Figure 3. Comparison of cumulative amount of ART in water permeated across silicone membrane using different concentrations of PVP.

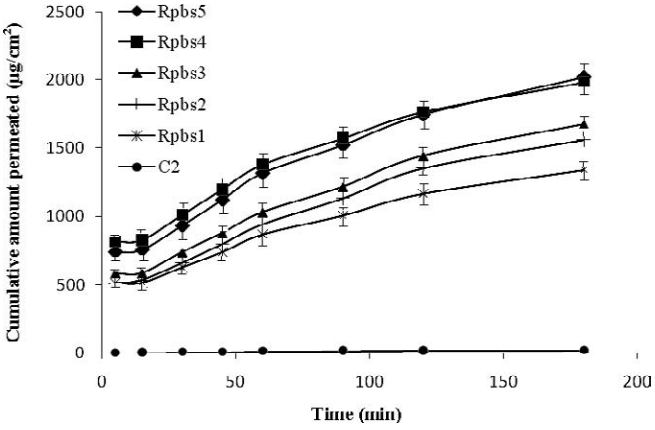

Figure 4. Comparison of cumulative amount of ART in PBS permeated across silicone membrane using different concentrations of PVP.

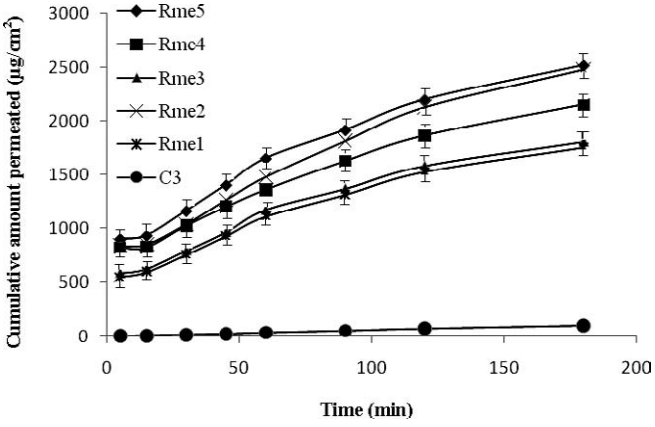

Figure 5. Comparison of cumulative amount of ART in methanol permeated across silicone membrane using different concentrations of PVP.

Table 2. Permeation Profile of Saturated Solutions of PM Ratios in Three Solvents[a]

PM Ratio	Flux (*J*) (μg/cm²/min)	Diffusion Coefficient ($10^{-4} \times D$) (cm²/min)	Permeability Coefficient ($10^{-4} \times K_p$) (cm/min)	Enhancement Ratio ER(J)
C_1	0.12 ± 0.004	0.959 ± 0.60	93.80 ± 3.53	-
R_{w1}	5.39 ± 0.03	13.26 ± 0.29	26.98 ± 0.13	44.61
R_{w2}	6.69 ± 0.10	10.70 ± 0.12	33.48 ± 0.50	55.34
R_{w3}	6.83 ± 0.03	10.75 ± 0.20	34.12 ± 0.16	56.44
R_{w4}	8.48 ± 0.42	12.62 ± 0.41	42.40 ± 2.12	70.09
R_{w5}	9.97 ± 0.30	10.66 ± 0.89	49.85 ± 1.51	82.41
C_2	0.10 ± 0.006	1.810 ± 1.43	65.60 ± 4.15	-
R_{pBs1}	5.06 ± 0.03	12.84 ± 0.57	25.32 ± 0.16	49.26
R_{pBs2}	6.39 ± 0.03	10.06 ± 0.16	31.96 ± 0.14	62.22
R_{pBs3}	6.67 ± 0.27	10.89 ± 0.33	33.40 ± 0.14	64.94
R_{pBs4}	7.11 ± 0.30	15.09 ± 0.78	35.60 ± 1.52	69.23
R_{pBs5}	7.76 ± 0.04	12.33 ± 0.38	38.75 ± 0.20	75.57
C_3	0.564 ± 0.02	0.666 ± 0.13	34.50 ± 1.41	-
R_{me1}	7.270 ± 0.05	10.05 ± 0.19	36.35 ± 0.27	12.89
R_{me2}	10.11 ± 0.05	10.15 ± 0.20	50.55 ± 0.29	17.92
R_{me3}	7.410 ± 0.01	10.50 ± 0.13	37.06 ± 0.06	13.14
R_{me4}	8.120 ± 0.49	12.83 ± 1.42	40.62 ± 2.49	14.40
R_{me5}	9.810 ± 0.07	12.06 ± 0.23	49.06 ± 0.34	17.40

[a]*Results are presented as mean ± SD (n = 3).*

In Vitro Permeation Studies

The steady-state flux was determined from the slope of the linear portion of the cumulative amount of permeation through silicone membrane versus time plot (during a course of 180 min), as shown in Figures 3–5. By applying Fick's laws of diffusion, permeability and diffusion coefficients were calculated. The values of the permeation parameters are summarized in Table 2. The permeation profiles for individual data were linear with an R^2 range of 0.95–0.99.

With an increase in the concentration of PVP–K30, the permeability coefficient increased as shown in Table 2. There were no statistically significant differences ($p > 0.05$) between the permeability coefficient values obtained for saturated solutions of PMs in all three solvents.

Table 3. Input Rates (μg/min) of ART from Saturated Solutions of PM Ratios in Three Solvents[a]

Sample	Water	PBS	Methanol
C	0.01 ± 0.003	0.08 ± 0.005	0.45 ± 0.02
R_1	4.25 ± 0.02	3.99 ± 0.02	5.73 ± 0.04
R_2	5.28 ± 0.07	5.04 ± 0.02	7.96 ± 0.04
R_3	5.38 ± 0.02	5.26 ± 0.02	5.84 ± 0.01
R_4	6.68 ± 0.34	5.61 ± 0.24	6.40 ± 0.39
R_5	7.86 ± 0.23	6.12 ± 0.03	7.74 ± 0.05

[a] *Results are presented as mean ± SD (n = 3).*

The diffusion coefficients obtained for the PMs in methanol show a trend of increasing order with increasing enhancer concentration. The diffusion coefficient values obtained for the PMs in water and PBS are erratic, as described in Table 2.

The enhancement ratio ER(J) was calculated by dividing the flux of each PM ratio by that of the control. The ER(J) values obtained are listed in Table 2. The order of enhancement ratios increased as the ratios increased (i.e., 1:0.5 < 1:1 < 1:2 < 1:4 < 1:9). This trend was seen in all three solvent systems examined, although the ER(J) values for PMs in methanol were much less than those for PMs in water and PBS. This is illustrated in Figures 6–8.

The input rate of the drug from its saturated solutions in water, PBS, and methanol was calculated. The data in Table 3 shows that the input rate was increased with increase in the concentration of PVP.

The experimental outcomes show that the silicone membrane was permeable to pure ART. The percutaneous absorption might be described by zero-order kinetics during the time of study (*9*). The concentration of enhancer in the system under investigation can influence the permeation of transdermal drug delivery (*14*, *15*). Thus, the amount of permeation enhancer present in the skin is an important factor in the enhancing effect (*16*). The input rate of permeant increased with an increase in PVP–K30 concentration, which could be due to the increase in the solubility of ART. Hence, an increased amount of ART was available at the surface of the membrane to be permeated, which agrees with the previous study (*9*).

The solvents used were all deliberately saturated with the PMs with a sufficient excess of solute (ART) to maintain a constant donor concentration throughout the course of the experiment in all cases investigated. Under equilibrium conditions, the flux is maximized when the outer layer of the membrane is saturated with the solute. The saturated solubility of a solute in a vehicle is related to that in the membrane by $C_{vehicle} = C_{membrane}/K$, where K is the partition coefficient. Hence, if $C_{membrane}$ is to remain constant, the product $KC_{vehicle}$ must stay constant. Thus, in an ideal situation, all saturated solutions of the same permeant in any solvent system should produce an equal flux through a membrane that is independent of solute concentration. Examination of the values in Table 2 reveals that the flux across the silicone membrane was not constant. Instead, it increased with an increase in the concentration of PVP–K30. This may be because some or all of the situations examined here were not ideal (i.e., there may be some interaction between the vehicle and membrane that increased the product of $KC_{vehicle}$ or diffusion coefficient of solute in the membrane) (*17*). It was also noticed that flux was the highest for the saturated solution of R_{me2}. This might be due to the enhancing effect of methanol itself (*14*).

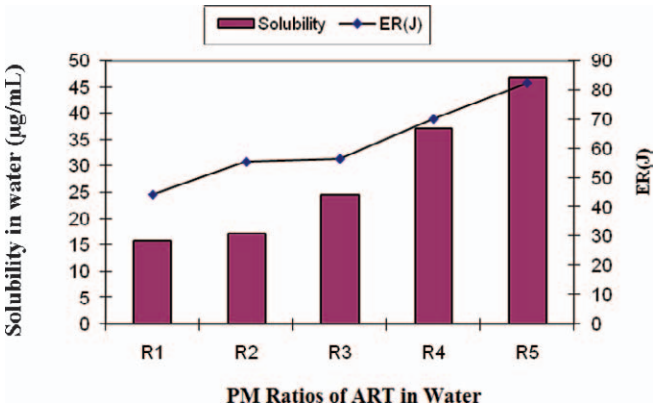

Figure 6. Graphical representation of solubility and ER(J) in water.

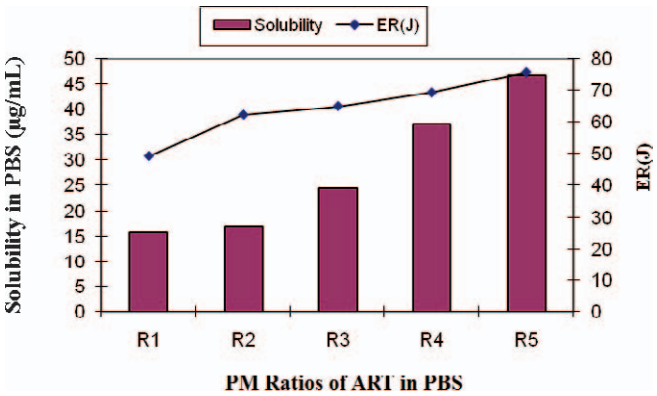

Figure 7. Graphical representation of solubility and ER(J) in PBS.

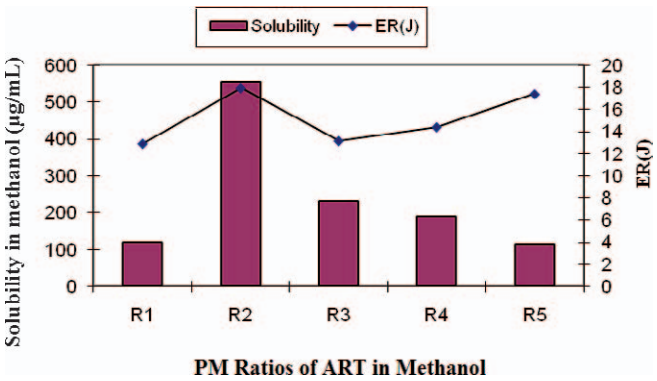

Figure 8. Graphical representation of solubility and ER(J) in methanol

The flux increased considerably with an increase in the concentration of PVP–K30 in PM ratios and was highest in R_5. For solvents that are less permeable like water and PBS, ER(J) was significantly higher as compared with the solvent that is more permeable, for which ER(J) was low. ANOVA shows no statistically significant differences in the values of K_p for PM ratios in all three solvents. ANOVA also confirmed that there was no significant difference in ER(J) for the PMs in water and PBS with respect to each other, while the reverse was true for PMs in methanol with respect to the other two solvent systems. The lack of ER(J) in methanol is related to the fast diffusion of methanol (acting as an enhancer itself) through the silicone membrane. Because of this flux, methanol would deplete quickly from the residual phase and from the membrane, thus increasing the drug concentration and possibly inducing drug crystallization inside the membrane (*18*, *19*). Conversely, saturated solutions in water and in PBS have lower flux through the membrane, except for R_{w4} and R_{w5} where the flux was a bit higher than the same ratios in methanol. Therefore, less solvent diffuses across the silicone membrane thus maintaining the drug solution before and inside the membrane.

CONCLUSION

The present study provides a detailed in vitro permeation study of the model drug ART using a silicone membrane. PVP is an effective enhancer of solubility and permeation of ART from the different PMs in various solvents. The enhancing effect of PVP is due not only to the change in the solubility of PMs in the solvent system, but to the transport rate of the permeant. There was no statistically significant difference ($p > 0.05$) in the permeability coefficient for ART from its PMs. The ER(J) was significantly different for all PMs as compared with the control. The results presented here now need to be confirmed with respect to clinical relevance, and an infinite dose of the drug used should be replaced with finite amount (therapeutic dose).

ACKNOWLEDGMENTS

The authors thank Hamaz Pharmaceuticals (Pvt.) Ltd., Multan, for its laboratory facility and HEC for the financial support to conduct this research project.

REFERENCES

1. Stoughton, R. B. Percutaneous absorption. *Toxicol. Appl. Pharmacol*. **1965**, *7* (Suppl. 2), 1–6.
2. Barry, B. W. Skin Transport. In *Dermatological Formulations Percutaneous Absorption*; Marcel Dekker: New York, 1983; pp 95–126.
3. Sinha, V. R.; Kaur, M. P. Permeation Enhancers for Transdermal Drug Delivery. *Drug Dev. Ind. Pharm*. **2000**, *26* (11), 1131–1140.
4. Thaithong, S.; Beale, G. H. Susceptibility of Thai isolates of Plasmodium falciparum to artemisinine (qinghaosu) and artemether. *Bull. World Health Organ*. **1985**, *63* (3), 617–619.
5. Klayman, D. L. Qinghaosu (artemisinin): an antimalarial drug from china. *Science* **1985**, *228* (4703), 1049–1055.
6. Titulaer, H. A. C.; Zuidema, J.; Kager, P. A.; Wetsteyn, J. C. F. M.; Lugt, C. B.; Merkus, F. W. H. M. The pharmacokinetics of artemisinin after oral, intramuscular and rectal administration to volunteers. *J. Pharm. Pharmacol*. **1990**, *42* (11), 810–813.
7. Akbuga, J.; Gursory, A.; Kendi, E. The Preparation and Stability of Fast Release Furosemide–PVP Solid Dispersion. *Drug Dev. Ind. Pharm*. **1988**, *14* (10), 1439–1464.
8. Margarit, M. V.; Marín, M. T.; Contreras, M. D. Solubility of Solid Dispersions of Pizotifen Malate and Povidone. *Drug Dev. Ind. Pharm*. **2001**, *27* (6), 517–552.
9. El-Badry, M.; Fathy, M. Enhancement of the Dissolution and Permeation Rates of Meloxicam by Formation of Its Freeze-dried Solid Dispersions in Polyvinylpyrrolidone K–30. *Drug Dev. Ind. Pharm*. **2006**, *32* (2), 141–150.
10. Ansari, M. T.; Iqbal, I.; Sunderland, V. B. Dihydroartemisinin–cyclodextrin complexation: Solubility and stability. *Arch. Pharm. Res*. **2009**, *32* (1), 155–165.
11. Zhao, S.-S.; Zeng, M.-Y. Spektrometrische Hochdruck-Flüssigkeits-Chromatographische (HPLC) Untersuchungen zur Analytic von Qinghaosu. *Planta Med*. **1985**, *51* (3), 233–237.
12. Franz, T. J. Percutaneous absorption on the relevance of in vitro data. *J. Invest. Dermatol*. **1975**, *64* (3), 190–195.
13. Cross, S. E.; Pugh, W. J.; Hadgraft, J.; Roberts, M. S. Probing the Effect of Vehicles on Topical Delivery: Understanding the Basic Relationship Between Solvent and Solute Penetration using Silicone Membranes. *Pharm. Res*. **2001**, *18* (7), 999–1005.
14. Duracher, L.; Blasco, L.; Hubaud, J. C.; Vian, L.; Marti–Mastres, G. The influence of alcohol, propylene glycol and 1,2-pentanediol on the permeability of hydrophilic model drug through excised pig skin. *Int. J. Pharm*. **2009**, *374* (1–2), 39–45.
15. Chow, D. S. L.; Kaka, I.; Wang, T. I. Concentration-dependent enhancement of 1–dodecylazacycloheptan-2-one on the percutaneous penetration kinetics of triamcinolone acetonide. *J. Pharm. Sci*. **1984**, *73* (12), 1794–1799.
16. Huang, Y. B.; Wu, P. C.; Ko, H. M.; Tsai, Y. H. Cardamom oil as a skin permeation enhancer for indomethacin, piroxicam and diclofenac. *Int. J. Pharm*. **1995**, *126* (1), 111–117.

17. Watkinson, A. C.; Joubin, H.; Green, D. M.; Brain, K. R.; Hadgraft, J. The influence of vehicle on permeation from saturated solutions. *Int. J. Pharm*. **1994**, *121* (1), 27–36.
18. Trottet, L.; Merly, C.; Mirza, M.; Hadgraft, J.; Davis, A. F. Effect of finite doses of propylene glycol on enhancement of in vitro percutaneous permeation of loperamide hydrochloride. *Int. J. Pharm*. **2004**, *274* (1–2), 213–219.
19. Watkinson, R. M.; Herkenne, C.; Guy, R. H.; Hadgraft, J.; Oliveira, G.; Lane, M. E. Influence of Ethanol on the Solubility, Ionization and Permeation Characteristics of Ibuprofen in Silicone and Human Skin. *Skin Pharmacol. Physiol*. **2009**, *22* (1), 15–21.